Circularly Polarized Shared Aperture K-band Transmitarray and Beamforming S-Band Patch Antenna Array

Serup, Daniel E.; Zhang, Shuai; Pedersen, Gert Frølund

Published in:
2023 17th European Conference on Antennas and Propagation (EuCAP)

DOI (link to publication from Publisher):
10.23919/EuCAP57121.2023.10133679

Publication date:
2023

Document Version
Accepted author manuscript, peer reviewed version

Circularly Polarized Shared Aperture K-band Transmitarray and Beamforming S-Band Patch Antenna Array

Daniel E. Serup *, Shuai Zhang (sz@es.aau.dk) *, and Gert Frølund Pedersen *.
* Department of Electronic Systems, Technical Faculty of IT and Design, Aalborg University, Denmark.

***Abstract*—This paper presents a circularly polarized shared aperture antenna. The proposed antenna is a combined S-band patch antenna array and a K-band transmitarray antenna. The high-frequency transmitarray feed and the low-frequency patch antenna array share the same aperture area. The high-frequency transmitarray surface only uses a single substrate layer and is electrically transparent to the low-frequency antenna part. With an impressive frequency-ratio of 5.55 and a radiating area of only 10x10 cm the antenna achieves an impedance bandwidth of more than 1 GHz and 5 GHz, and a peak realized gain of 15.35 dBi and 22.85 dBi, in the S- and K-band respectively. Additionally, the low-frequency antenna mode shows a good beamforming performance with a 120-degree steering range with only a 1.25 dB gain variation.**

***Index Terms*—Antenna, Transmitarray, Patch Antenna Array, Circular Polarization, Dual-band, Shared Aperture, S-band, K-band, mm-wave, Beam-steering, Beamforming.**

I. Introduction

Dual-band and shared aperture antennas are an interesting and widely popular topic for both academic researchers and for industry professionals. For space applications, dual-band antennas with a high frequency-ratio dual-band operating are often desired. With dual S- and K-band frequency operation a satellite antenna can transmit and receive simultaneously. The high-frequency mode allows for a high-speed communication down-link and the low-frequency mode enables a simultaneous communication up-link connection. This configuration is especially interesting for Low-earth satellite applications as these satellites only have very short windows for communication with each orbit. Commonly for Satellite-Earth communication links, is the requirement that the used antennas should be circularly polarized. Circular polarized satellite antennas are utilized to mitigate the polarization shift of the atmosphere and thus eliminate polarization mismatch and gain loss.

Different use cases and applications set different requirements for the performance and features of antennas [1]–[12]. Transmitarray antennas are often reported in the literature to yield features such as; high gain, dual-band, and circular polarization. For this paper, a high frequency-ratio dual-band antenna with circular polarization is desired. Additionally, the antenna should have low-frequency beam-forming capabilities. Some of the antennas reported in the literature satisfy parts of the requirements, but unlike the antenna presented in this paper, none of them satisfies all the listed requirements simultaneously. [13]–[21].

In [1] a shared aperture dual-band transmitarray antenna for S- and Ka-Band is presented. The antenna is a combination of a low-frequency patch antenna array and a high-frequency Transmitarray. A comparison with the state-of-the-art literature shows that this antenna is unique since it achieves good performance in two frequency bands with a high separation factor, in addition to enabling low-frequency beamforming. However, the antenna lacks the critical feature of circular polarization. The work of this paper will expand upon the work presented in [1] by modifying the antenna to achieve circular polarization in both frequency bands.

II. Antenna configuration

Different views of the proposed antenna simulation model are seen in Fig. 1. The figures show the full simulation model and different close-up pictures of the feeds and the unit element. As seen from the figures the suggested antenna has two parts. The bottom part contains the high-frequency feed and the low-frequency antenna array. The top part houses the high-frequency unit elements. The remaining part of this section will give a detailed description of the individual parts of the antenna, starting with the high-frequency unit element followed by the high-frequency feed antenna, and lastly, the section will conclude with a description of the low-frequency antenna mode.

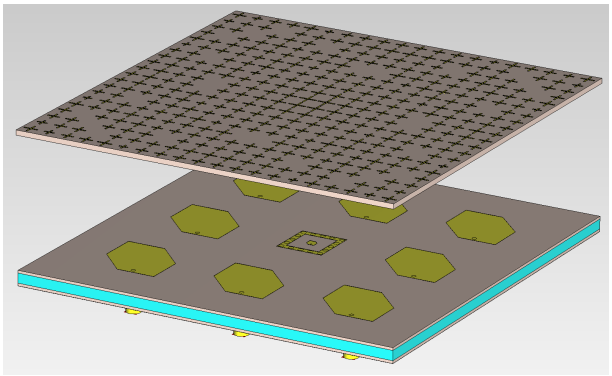

(a)

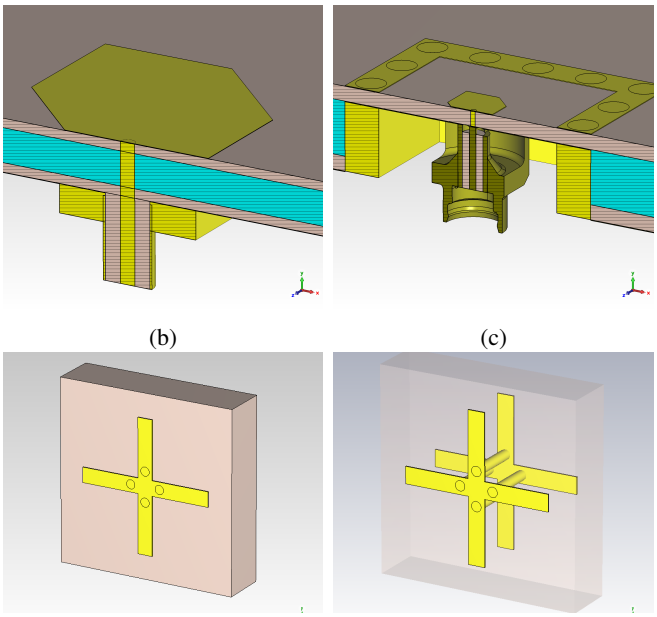

(b) (c)

(d) (e)

Fig. 1: Simulation model of the antenna. (a) Full simulation model. (b) Low-frequency feed. (c) High-frequency feed. (d & e) Unit element.

The designed and used high-frequency unit element is seen in figures 1d and 1e. The unit elements are printed on a single substrate layer to realize good low-frequency transparency. The unit element consists of two cross shapes printed on each side of the substrate layer. The two opposite crosses are connected by four VIA pins to increase the coupling between the two crosses on each side of the substrate. To change the phase transmission behavior of the unit element, the length of the cross is altered. In Fig. 2 the magnitude and phase of the transmission coefficient of the unit element for different element sizes are seen. The plots have multiple curves for different frequencies and incident angles. At 4.5 GHz the unit element has a flat phase response and a low loss. This indicates good transparency of the unit element at the lower center frequency of 4.5 GHz. At 25 GHz, the simulation shows that the transmission phase is tunable in a 330° range with a low loss of less than 2.5 dB.

An additional simulation is conducted for the unit element. Fig. 3 shows the magnitude and phase response of the unit element transmission coefficient for a wide frequency range. In Fig. 3a, It is seen how the phase of the unit element is not affected by the unit element size for frequencies below 20 GHz. Fig. 3b shows that the magnitude of the unit element transmission coefficient is lower than 1-dB for frequencies below 7 GHz. These simulation results show that the low-frequency mode has a high degree of freedom and could easily be tuned to a different frequency simply by tuning the resonance frequencies of the low-frequency antenna array.

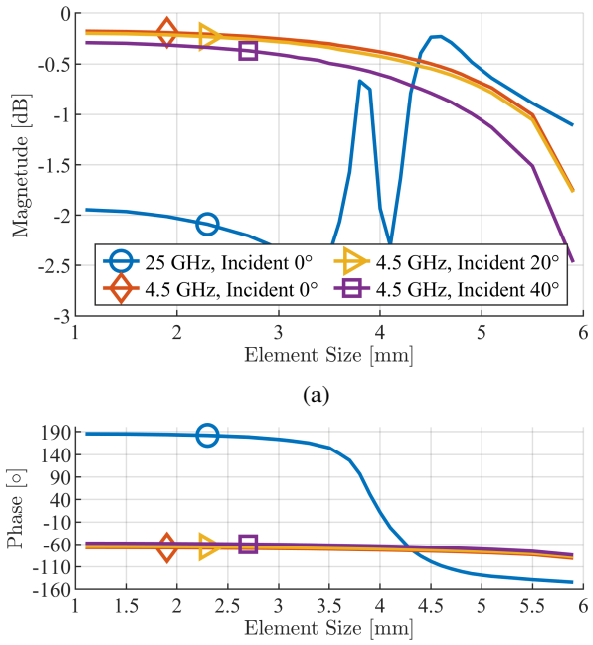

Fig. 2: Simulated transmission coefficient of the designed unit element for different element sizes. (a) Magnitude response. (b) Phase response.

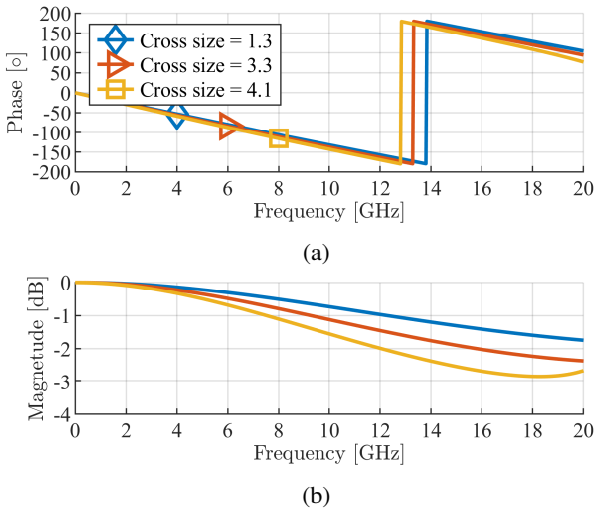

Fig. 3: Simulated transmission coefficient of the designed unit element for a wide frequency range. (a) Magnitude response. (b) Phase response.

The high-frequency feed of the proposed antennas is a simple patch antenna. It achieves circular polarization by having two opposite corners truncated and being fed in the diagonal. To achieve a suitable distance between the feeding patch element and the ground plane the feeding patch antenna needs its own small ground plane. This ground plane is placed on the bottom of the topmost of the three layers. The two

bottom layers have square cutaways to allow space for a connector. The high-frequency feed is surrounded by a printed copper square annular ring to shield it from surface waves. The ring is connected to the ground plane with multiple VIAs. The ground plane for the high-frequency feed is connected to the low-frequency ground plane at the bottom of the lower layer to ensure a connected and continuous ground. A picture of the implemented high-frequency feed is seen in Fig. 1c. A model of the high frequency in an isolated scenario is seen in Fig. 4a, and its simulated performance is seen in 4b

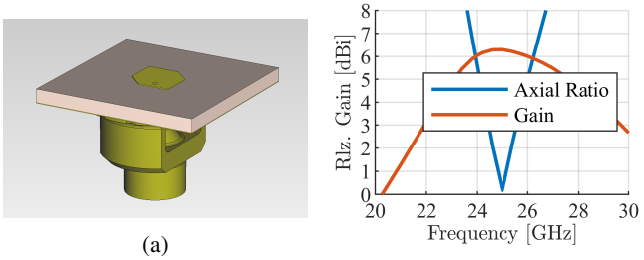

(a) (b)

Fig. 4: The high-frequency feed (a) Simulation model. (b) Simulated performance.

The low-frequency antenna array is a 3 by 3 grid configuration but with the center element removed to allow for space for the high-frequency feed. this array achieves circular polarization since two opposite corners of each patch have been trimmed. To improve the impedance bandwidth of the low-frequency antenna operation the separation between the low-frequency patch antenna and the ground plane has been enlarged by adding a 3 mm PP layer in between the two substrate layers. A single isolated low-frequency unit element is seen in Fig. 5a and it simulated realized circularly polarized gain and axial-ratio is seen in Fig. 5b.

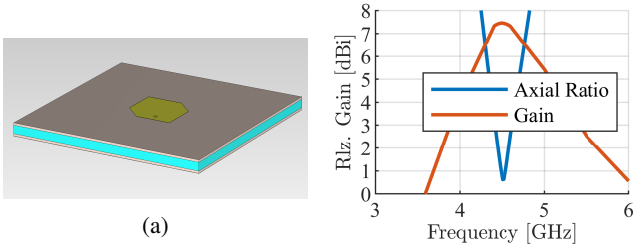

(a) (b)

Fig. 5: The Low-frequency feed (a) Simulation model. (b) Simulated performance.

The low-frequency antenna array achieves beamforming capabilities by supplying each antenna element with a phased input signal. The low-frequency patch antenna elements have a center-to-center separation of 35 mm. This distance is calculated using $d = \frac{\lambda}{1 + sin(\theta)}$. The selected distance aims at a scanning range of $\pm 60^{\circ}$ without grating lobes.

Tab. I summarizes the dimensions and design parameters of the proposed antenna design.

TABLE I: The dimensions and parameters of the proposed antenna design.

Parameter	***Value***
Substrate type	Rogers RO4003
Substrate height	0.812 mm
Dialectic constant	3.55
Middle layer material	Polypropylen
Middle layer height	3 mm
Middle layer dialectic constant	2.245
Board size	100 mm
Board Separation	40 mm
Low-frequency part	
Untrimmed patch size	18.81 mm
Patch Corner Trim	8.72 mm
Feeding point z (Distance from center)	6.72 mm
Feeding point x (Distance from center)	2.38 mm
Feed pin diameter	1.27 mm
Ground cut out diameter	4.22 mm
Antenna separation	35 mm
High-frequency part	
Untrimmed patch size	2.89 mm
Patch corner trim	1.36 mm
Feeding point z (Distance from center)	0.95 mm
Feeding point x (Distance from center)	0.33 mm
Feed pin diameter	0.30 mm
Ground cut diameter	1.23 mm
Solder pad diameter	0.60 mm
Unit element separation	6 mm
Unit element size	1.3 - 5.9 mm
Cross Width	0.50
Pin Radius	0.15
Pin Position (From Center)	0.50

III. Simulation Results

In this section, the simulated performance of the proposed transmitarray will be presented. The performance of the antenna will be evaluated and in some cases will be compared with two reference antennas. The reference antennas are seen in Fig. 6. The low-frequency reference is a version of the proposed antenna without the high-frequency surface. The high-frequency reference is a version of the antenna without the low-frequency patch antenna array.

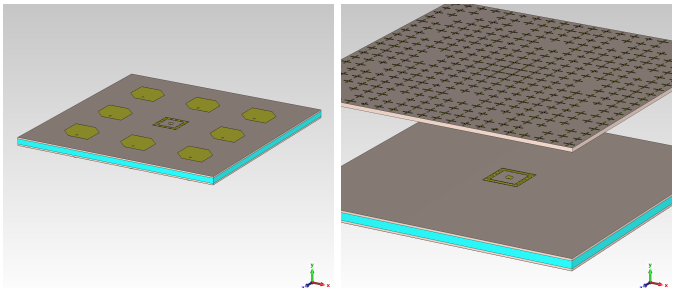

(a) (b)

Fig. 6: Reference antenna simulation models. (a) Low-frequency reference. (b) High-frequency reference.

Fig. 7 shows the S-parameters of the low-frequency part of the antenna. It is seen how the impedance match is very good as the -10db impedance bandwidth is more than 1 GHz. Additionally, it is seen how the low-frequency inter-element coupling is below -16 dB in the full frequency range. With the highest coupling being S6,5 peaking at 4.2 GHz. Lastly, the bottom plot shows that the low- to high-frequency coupling is below -40 db for all antenna ports.

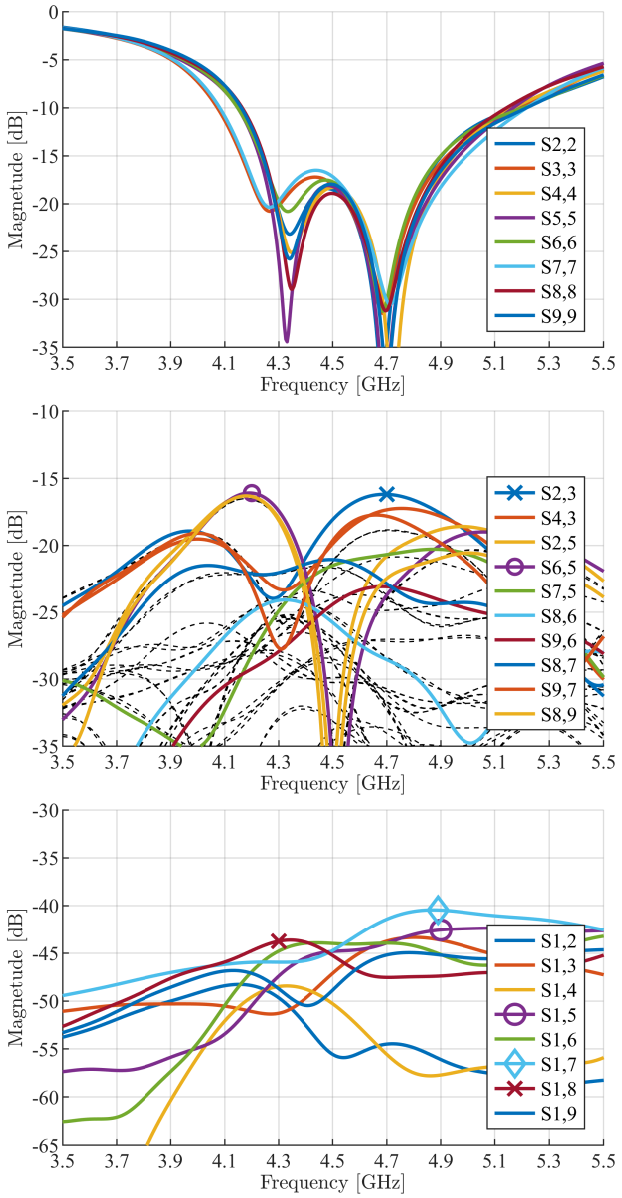

Fig. 7: Simulated low-frequency S-parameters of the proposed antenna.

The S-parameters of the high-frequency mode is shown in Fig. 8. Here an impedance bandwidth greater than 5 Ghz and a maximum coupling of -27 dB is observed.

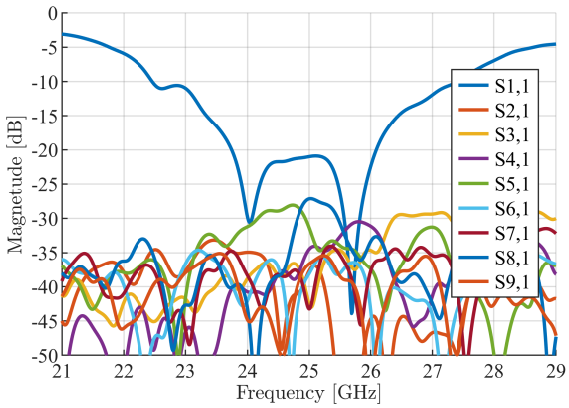

Fig. 8: Simulated high-frequency S-parameters of the proposed antenna.

The simulated radiation patterns of the proposed antenna is seen in Fig. 9. Fig. 9a shows that low-frequency antenna part is able to achieve a realized gain of 15.30 dBi at 4.5 GHz. Fig. 9b shows that the transmitarray part of the prototype antenna achieves a realized gain of 22.60 dBi at 25 GHz.

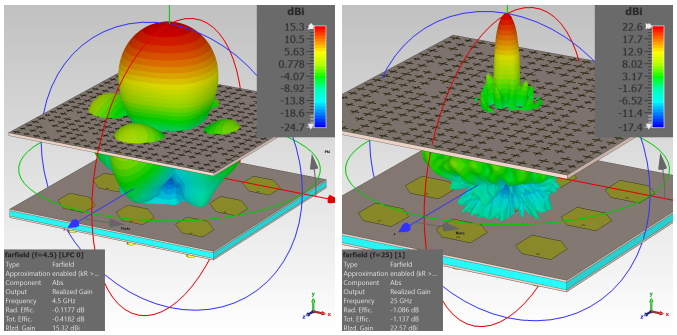

(a) (b)

Fig. 9: Simulated radiation pattern. (a) Low-frequency mode at 4.5 GHz. (b) High-frequency mode at 25 GHz.

The beamforming performance of the proposed antenna compared with the reference antenna is seen in Fig. 10. Good agreement between the two antennas is observed. However with a 0.8 dB gain advantage for the proposed antenna. The proposed antenna only has a 1.25 dB gain variation when scanning in a 120° range.

The boresight realized circularly polarized gain and axial-ratio of the two frequency modes of the antenna is seen in figures 11 and 12. In both cases, a comparison with the reference antennas is made. It is seen how the high-frequency modes of the antenna match the reference simulations almost identically. Furthermore, the low-frequency mode is also very similar to its reference simulation which shows the good electrically transparency of the transmitarray surface in the low-frequency band. The peak circularly polarized realized gain in the two cases is 15.35 and 22.85 dB. The 3 dB axial ratio bandwidth in the two cases is 600 MHz and 1.1 GHz.

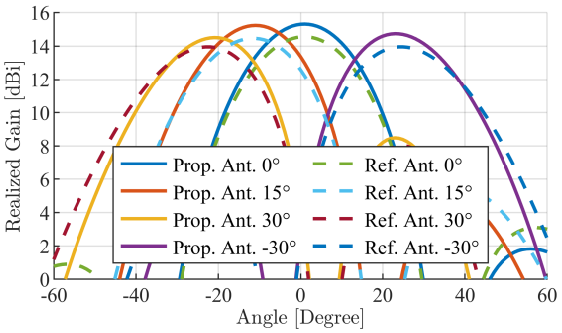

Fig. 10: Simulated low-frequency beamforming performance.

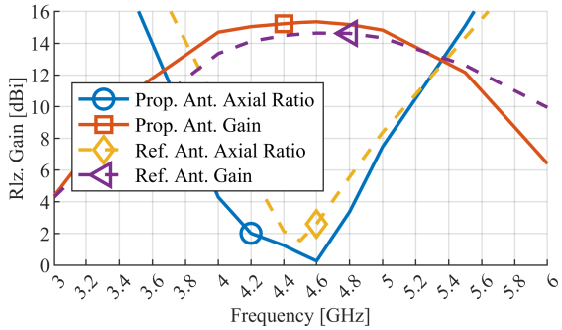

Fig. 11: Realized circularly polarized gain and axial ratio of the low-frequency mode in the boresight direction.

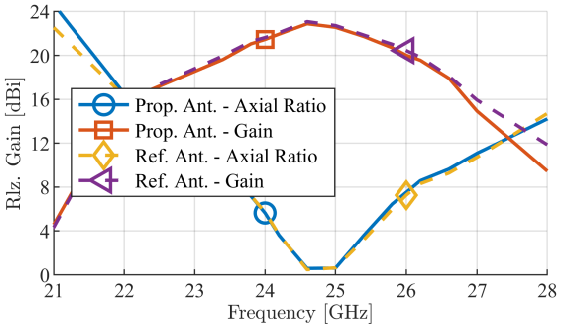

Fig. 12: Realized circularly polarized gain and axial ratio of the high-frequency mode in the boresight direction.

IV. Conclusion

A shared aperture dual-band antenna has been designed successfully. The antenna is a combined K-band transmitarray and a beamforming capable patch antenna array for S-band. The antenna achieves good circular polarization and low axial ratio for both frequency bands. The proposed antenna achieves impedance bandwidths of more than 1 GHz and 5 GHz, and realized gains of 15.3 dBi and 22.6 dBi, at 4.5 GHz and 25. GHz, respectively. Additionally, the proposed antenna is shown to only have a 1.25 dB gain drop-off in a 60-degree beam-steering range. The design and unique features of the presented antenna make it interesting for many new and different applications such as satellite communication.

References

[1] D. E. Serup, G. F. Pedersen and S. Zhang, "Combined Single-Layer K-Band Transmitarray and Beamforming S-Band Antenna Array for Satcom," *IEEE Open Journal of Antennas and Propagation,* vol. 3, pp. 1134-1140, 2022.

[2] T. Li and Z. N. Chen, "Shared-Surface Dual-Band Antenna for 5G Applications," *IEEE Trans. Antennas Propag.,* vol. 68, no. 2, pp. 1128-1133, Feb. 2020.

[3] F. Qin et al., "A Simple Low-Cost Shared-Aperture Dual-Band Dual-Polarized High-Gain Antenna for Synthetic Aperture Radars," *IEEE Trans. Antennas Propag.,* vol. 64, no. 7, pp. 2914-2922, July 2016.

[4] A. I. Sandhu, E. Arnieri, G. Amendola, L. Boccia, E. Meniconi and V. Ziegler, "Radiating Elements for Shared Aperture Tx/Rx Phased Arrays at K/Ka Band," *IEEE Trans. Antennas Propag.,* vol. 64, no. 6, pp. 2270-2282, June 2016.

[5] D. E. Serup, R. J. Williams, S. Zhang and G. F. Pedersen, "Shared Aperture Dual S- and X-band Antenna for Nano-Satellite Applications," *14th European Conference on Antennas and Propagation (EuCAP),* 2020

[6] D. E. Serup, R. J. Williams, S. Zhang and G. F. Pedersen, "Dual S- and X-Band Shared Aperture Antenna for Nano-Satellite Applications," *15th European Conference on Antennas and Propagation (EuCAP),* 2021

[7] R. Deng, F. Yang, S. Xu and M. Li, "An FSS-Backed 20/30-GHz Dual-Band Circularly Polarized Reflectarray With Suppressed Mutual Coupling and Enhanced Performance," *IEEE Trans. Antennas Propag.,* vol. 65, no. 2, pp. 926-931, Feb. 2017.

[8] C. Han, J. Huang and Kai Chang, "A high efficiency offset-fed X/ka-dual-band reflectarray using thin membranes," *IEEE Trans. Antennas Propag.,* vol. 53, no. 9, pp. 2792-2798, Sept. 2005.

[9] Y. Chen, L. Chen, H. Wang, X. Gu and X. Shi, "Dual-Band Crossed-Dipole Reflectarray With Dual-Band Frequency Selective Surface," *IEEE Antennas Wireless Propag. Lett.,* vol. 12, pp. 1157-1160, 2013.

[10] R. Shamsaee Malfajani and B. Abbasi Arand, "Dual-Band Orthogonally Polarized Single-Layer Reflectarray Antenna," *IEEE Trans. Antennas Propag.,* vol. 65, no. 11, pp. 6145-6150, Nov. 2017.

[11] D. E. Serup, G. F. Pedersen and S. Zhang, "Dual-Band Shared Aperture Reflectarray and Patch Antenna Array for S- and Ka-Band," *IEEE Trans. Antennas Propag.,* 2021.

[12] D. E. Serup, S. Zhang and G. F. Pedersen, "Circularly Polarized Shared Aperture Reflectarray and Patch Antenna Array for S- and Ka-Band," *16th European Conference on Antennas and Propagation (EuCAP)*, 2022

[13] K. Pham, R. Sauleau, E. Fourn, F. Diaby, A. Clemente and L. Dussopt, "K/Ka-band transmitarray antennas based on polarization twisted unit-cells," *12th European Conference on Antennas and Propagation (EuCAP),* 2018.

[14] Z. Zhang, X. Li, C. Sun, Y. Liu and G. Han, "Dual-Band Focused Transmitarray Antenna for Microwave Measurements," *IEEE Access,* vol. 8, pp. 100337-100345, 2020.

[15] R. Madi, A. Clemente and R. Sauleau, "Dual-Band Dual-Linearly Polarized Transmitarray at Ka-Band," *50th European Microwave Conference (EuMC),* 2021, pp. 340-343.

[16] Q. Luo, S. Gao, M. Sobhy and X. Yang, "Wideband Transmitarray With Reduced Profile," *IEEE Antennas Wireless Propag. Lett.,* vol. 17, no. 3, pp. 450-453, March 2018.

[17] X. Yi, T. Su, B. Wu, J. Chen, L. Yang and X. Li, "A Double-Layer Highly Efficient and Wideband Transmitarray Antenna," *IEEE Access,* vol. 7, pp. 23285-23290, 2019.

[18] P. Naseri, S. A. Matos, J. R. Costa, C. A. Fernandes and N. J. G. Fonseca, "Dual-Band Dual-Linear-to-Circular Polarization Converter in Transmission Mode Application to K/Ka -Band Satellite Communications," *IEEE Trans. Antennas Propag.,* vol. 66, no. 12, pp. 7128-7137, Dec. 2018.

[19] P. -Y. Feng, S. -W. Qu, X. -H. Chen and S. Yang, "Low-Profile High-Gain and Wide-Angle Beam Scanning Phased Transmitarray Antennas," *IEEE Access,* vol. 8, pp. 34276-34285, 2020.

[20] M. Jiang, Z. N. Chen, Y. Zhang, W. Hong and X. Xuan, "Metamaterial-Based Thin Planar Lens Antenna for Spatial Beamforming and Multibeam Massive MIMO," *IEEE Trans. Antennas Propag.,* vol. 65, no. 2, pp. 464-472, Feb. 2017.

[21] F. Diaby, A. Clemente, R. Sauleau, K. T. Pham and L. Dussopt, "2 Bit Reconfigurable Unit-Cell and Electronically Steerable Transmitarray at Ka -Band," *IEEE Trans. Antennas Propag.,* vol. 68, no. 6, pp. 5003-5008, June 2020.